AAPS PharmSciTech, Vol. 15, No. 5, October 2014 (© 2014)
DOI: 10.1208/s12249-014-0153-4

Research Article

An Epichlorohydrin-Crosslinked Semi-Interpenetrating GG-PEO Network as a Xerogel Matrix for Sustained Release of Sulpiride

Famida G. Hoosain,[1] Yahya E. Choonara,[1] Pradeep Kumar,[1] Lomas K. Tomar,[1] Charu Tyagi,[1] Lisa C. du Toit,[1] and Viness Pillay[1,2]

Received 14 February 2014; accepted 14 May 2014; published online 12 June 2014

Abstract. The current study involved the development of a novel sustained release crosslinked semi-IPN xerogel matrix tablet prepared by chemical crosslinking of poly(ethylene) oxide (PEO) and gellan gum (GG) employing epichlorohydrin (EPI) as crosslinker. A Box–Behnken design was employed for the statistical optimization of the matrix system to ascertain the ideal combination of native polymeric and crosslinking agents. Characterization studies were performed by employing standard polymer characterization techniques such as Fourier transform infrared spectrometry, differential scanning calorimetry, and scanning electron microscopy. Formulated matrix tablets displayed zero-order release kinetics, extending over 24 h. The mechanism of drug release was primarily by swelling and surface erosion. Crosslinked semi-IPN xerogel matrix tablets were compared to non-crosslinked polymer blends; results from the study conducted showed that the physiochemical properties of the PEO and GG were sufficiently modified to allow for sustained release of sulpiride with a 100% drug release at 24 h in a controlled manner as compared to non-crosslinked formulations which displayed further release beyond the test period. Crosslinked formulations displayed water uptake between 450 and 500% indicating a controlled rate of swelling and erosion allowing for sustained release. Surface morphology of the crosslinked system depicted a porous structure formed by interpenetrating networks of polymers, allowing for a greater degree of controlled penetration into the system affording it the ability to sustain drug release. Therefore, conclusively, based on the study performed, crosslinked PEO-GG allows for the sustained release of sulpiride from a hydrophilic semi-IPN xerogel matrix system.

KEY WORDS: epichlorohydrin; matrix tablet; semi-interpenetrating polymer network; sustained release; sulpiride.

INTRODUCTION

The use of hydrophilic matrix systems in order to achieve sustained drug delivery kinetics has been a widespread field of research studies in the pharmaceutical industry. The development of sustained release dosage forms is beneficial for the optimal therapeutic outcomes required for many disease states, which allows for improved patient compliance, and as an extension the safety and efficacy of drug therapy. There are various ways in which controlled release is achieved with regards to oral dosage forms. Amid the many approaches available, the most common is that of hydrophilic matrix systems due to their low-cost production, ability to modify, and closely control drug release kinetics [1], as well as define drug delivery according to desired release profile and improved patient compliance because of a fewer administrations by maintaining constant levels of drug within the circulatory system [2]. Sustained release systems allow for the modulation of drug delivery into circulation at predetermined time points depending on the release profile preferred, thereby sustained release formulations allow for optimum therapeutic outcomes, prolonged efficacy of drug molecule, and a reduction in toxicity profiles [3]. Natural polymers have been used with great recurrence lately for these very reasons. Natural polymers are readily available within the environment and thus they are cheap, they also undergo easy metabolism by naturally occurring enzymes thereby allowing for biodegradability and biocompatibility [4]. Among the many advantages of the use of natural polymer in the development of novel drug delivery systems is that they have no cytotoxic effects associated with the polymer or its products of degradation and are commonly considered safe as they are food grade materials. These naturally occurring polymers can undergo modification reactions as to allow for the enhancement of mechanical and release kinetic properties as per formulation requirements [5].

However, natural polymers are also subject to certain limitations, such as uncontrolled hydration rates and loss of viscosity on storage; it has been found that modifications such as crosslinking, blending and formation of interpenetrating polymer networks (semi-IPN) improve these limitations. In the current study, a semi-IPN has been used to modify the

[1] Wits Advanced Drug Delivery Platform Research Unit, Department of Pharmacy and Pharmacology, School of Therapeutic Sciences, Faculty of Health Sciences, University of the Witwatersrand, Johannesburg, 7 York Road, Parktown, 2193, South Africa.
[2] To whom correspondence should be addressed. (e-mail: viness.pillay@wits.ac.za)

undesirable limitations of the natural polymers employed such as GG. Semi-IPNs are combinations of two polymers, when at least one polymer network is crosslinked independently within the direct presence of the other polymer. When one of the polymers is crosslinked only it is known as a semi-IPN. It is found that in the formulation process of controlled release drug delivery systems the use of hydrophilic polymers is most prevalent due primarily to their low toxicity, low cost, biocompatibility, and biodegradability. Polysaccharides such as xanthan gum and guar gum are among the many hydrophilic polymers used [6]. The mechanism of drug release from hydrophilic polymer-based matrix systems encompasses water penetration, dissolution, polymer swelling, and polymer erosion. GG is a high molecular weight hydrophilic anionic deacetylated polysaccharide which is produced by the fermentation of *Shingomonas elodea*; the organism is aerobic, gram negative, and nonpathogenic. Its chemical structure consists of four linked monosaccharides, one molecule of rhamnose, one molecule of glucuronic acid, and two glucose molecules [7]. GG functions as a gelling agent in many foods and pharmaceutical products. Poly(ethylene oxide) is a nonionic water soluble polymer; research has shown that it is capable of retarding the release of drugs and thus its use in controlled release formulations is widespread. The mechanism of drug release from poly(ethylene oxide)-based delivery systems is centered on swelling and erosion of the polymer. The chemical structure consists of an epoxide ring; two corners of the molecule have $–CH_2$-links, with the third corner having oxygen. These poly(ethylene oxide) water soluble polymers may be crosslinked to form gels with great water retention properties. Poly(ethylene oxide) is nontoxic and biodegradable and thus well suited for use within the pharmaceutical scope of drug delivery systems [8].

Epichlorohydrin is an epoxide agent, which is a colorless, sweet chloroform smelling liquid at room temperature. It is used in the production of many synthetic materials as well as in the crosslinking of starch and in the production of pharmaceutical products [9]. Sulpiride (5-(aminosulfonyl)-N-f1-ethyl-2-pyrrolidinylgmethyl-2-methoxybenzamide) is a known selective dopamine D2 antagonistic activity, with both antipsychotic and antidepressant actions. It is effective in the treatment of psychological disorders such as schizophrenia, with the risk and occurrence of extrapyramidal side effects being low [10]. Sulpiride has been used commonly in the treatment of psychiatric disorders due to the anti-dopaminergic and anti-psychotic effects it exhibits. However, the use of sulpiride is usually associated with the need for high dosages to achieve the desired clinical outcome, which thereby leads to a reduction in patient compliance. In general, the hazard and intensity of side effects related to anti-psychotic drugs increase with a corresponding increase in dosage; furthermore, it has been stated that the risk of side effects also depends on the rate of drug delivery [11]. Sulpiride has a 'bell-shaped' partition pH profile which noticeably indicates that it is a highly hydrophilic and poorly lipophillic species at physiological pH and is greatly improbable to be partitioned into lipophillic media [12]. Sulpiride is soluble in acid medium (HCL 0.1 M), and organic solvents (ethanol) yet sparingly soluble in aqueous medium (distilled water) [13].

The aim of this study centers on the formulation of a semi-IPN polymer matrix for the incorporation of sulpiride so as to enable controlled bioactive release thereby ensuring improved patient compliance by reducing the in pill burden as well as enhancement of bioavailability.

MATERIALS AND METHODS

Materials

Gellan gum (GG) (Gelzan™CM, 119 K0090), poly(ethylene oxide) (PEO) (Polyox™, WSR303), (±) sulpiride, epichlorohydrin (EPI) 99% (E1055), carboxymethylcellulose sodium (CMC) (#08831KH), and magnesium stearate were purchased from Sigma Aldrich (Steinham, Germany), while acetone (58.08 assay, A101010) and sodium hydroxide (SAAR5823160EM, assay min. 97%) were purchased from Merck (Darmstadt, Germany).

Synthesis of Crosslinked Xerogel

Semi-interpenetrating polymer network (IPN) xerogels (semi-IPN xerogel) were synthesized in accordance with the Box–Behnken statistical experimental design system shown in Table I. Solutions of PEO of varying concentrations in distilled water were prepared ranging from 1–2.5%*w/v*; thereafter, a variation of weights of GG ranging between 3.7 and 7.4%*w/v* was added to the above mentioned solutions and allowed to stir on a magnetic stirrer at an intermediate speed. Once GG was appropriately dissolved, epichlorohydrin (EPI) was added dropwise allowing for a period of stirring between each drop, within a range of 2.9–5.9%*v/v* followed by further stirring with a magnetic stirrer for 30 min to allow for effective crosslinking to occur. The resulting viscous, slightly opaque gel was poured into a beaker of 200–500 mL acetone and allowed to precipitate for approximately 3 h. Thereafter, the precipitated gel was drained of all the excess acetone using a laboratory strain and placed in a petri dish, and air dried under fume hood for a further 24 h. The resultant xerogel is then crushed into a uniform powder using a mortar and pestle and electrical grinder for formulation of sustained release semi-IPN xerogel matrix tablets as depicted in Fig. 1.

Preparation of the Semi-IPN Xerogel Matrix Tablets

Semi-IPN xerogel matrix tablets were prepared consisting of a 100 mg sulpiride to 200 mg xerogel matrix using the direct compression method of preparation. All tablet excipients including xerogel with the exception of magnesium stearate were mixed in a geometric fashion for 5 min, after which magnesium stearate was added and mixed for a further 2 min. The dry blend of powdered excipients was directly compressed using a hand operated Carver Press tableting press (Model 3851–0, S/N 43000–904, Wabash, IN, USA) employing a pressure of 5 tons.

Characterization of the Semi-IPN Xerogel Matrix Tablets

Physiomechanical Evaluation of Fabricated Semi-IPN Xerogel Matrix Tablets

The matrix tablets of PEO-GG xerogel, GG, and PEO were evaluated by textural analysis studies to determine the

Table I. Box-Behnken Design Template for the Statistically Derived 15 Semi-IPN Xerogel Formulations and their Respective Chemical Compositions.

Crosslink Xerogel F#	PEO Concentration (%*w/v*)	GG Concentration (%*w/v*)	EPI-Crosslinker Volume (mL)	Mg^{+} Stearate Mass (mg)	CMC Mass (mg)
F1	2.5	7.35	0.6	1.5	12
F2	2.5	5.51	0.8	1.5	12
F3	1.75	5.51	0.6	1.5	12
F4	1.75	5.51	0.6	1.5	12
F5	1	5.51	0.8	1.5	12
F6	1	7.35	0.6	1.5	12
F7	1.75	7.35	0.4	1.5	12
F8	1	3.68	0.6	1.5	12
F9	1.75	7.35	0.8	1.5	12
F10	1.75	3.68	0.8	1.5	12
F11	1	5.51	0.4	1.5	12
F12	1.75	5.51	0.6	1.5	12
F13	2.5	3.68	0.6	1.5	12
F14	1.75	3.68	0.4	1.5	12
F15	2.5	5.51	0.4	1.5	12

physiomechanical properties of the tablets. Information such as hardness, deformation, rigidity, and resilience were thus obtained from the data collected from texture analysis. PEO-GG xerogel, GG, and PEO tablets, 3 mm in thickness, respectively, were evaluated from force *versus* distance and force *versus* time profiles generated on a TA. XT*plus* Texture Analyzer (Stable Microsystems, Surrey, UK) equipped with a 2 mm flat cylindrical probe, 5 kg load cell, and Texture Exponent (V3.2) software for processing of data. Matrix tablets were secured on a raised platform fitted with a 5-mm-diameter central hole. A central probe with a weight of 5 kg was lowered into the surface of the tablet [14], in accordance with the test parameters listed in Table II.

Brinell Hardness Number, Deformation, Rigidity, and Resilience Determination

The Brinell Hardness test was employed to determine the hardness of tablets where a load of 5 kg was applied to the surface of the tablets via a steel indenter of 3.175 mm in diameter. Thus, the diameters of the resultant indentation on the surface of the tablets were measured, and the Brinell Hardness Number (BHN) was calculated using Eq. 1.

$$\text{Brinell Hardness Number} = 2F/\left(\pi D\left(D-\left(D^2-d^2\right)\right)\right) \quad (1)$$

Where F is the load on the indenting tool (force generated in kg), D is the diameter of the spherical probe indenter (3.175 mm), and d is the diameter at the rim of the impression made (depth 0.5 mm) [15].

Deformation and rigidity were determined from evaluating the area under the curve (AUC) as well as the gradient from the force *versus* distance graph.

By plotting a force *versus* time graph the values for 1:2 and 2:3 were obtained, thereby resilience may then be calculated when a strain of 10% is applied with the use of Eq. 2.

$$\text{Resilience} = \left(\frac{2:3}{1:2}\right) \times 100 \quad (2)$$

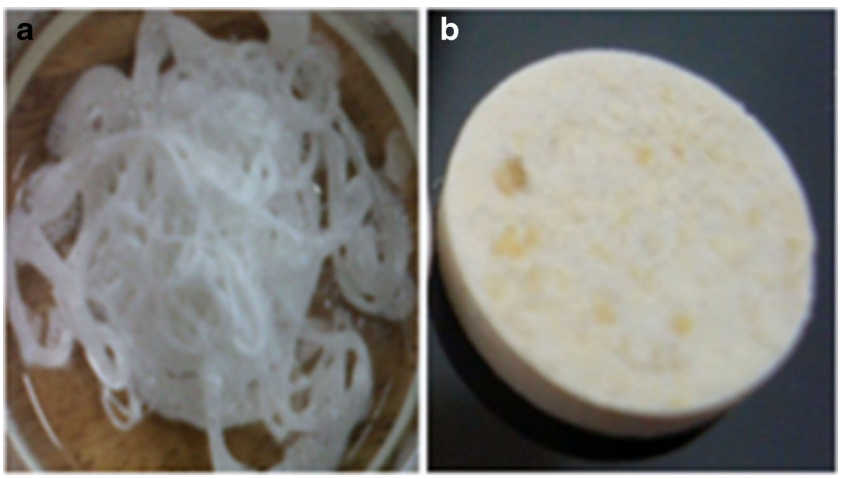

Fig. 1. Digital images of semi-IPN xerogel after precipitation in acetone at 3 h (**a**) and semi-IPN xerogel polymer matrix tablets compressed employing the *Carver Press 3851–0* (**b**)

Table II. Test Parameters used During Texture Analysis as per Standard Protocol for Solid Dosage Forms.

Parameters	Test Settings
Test mode	Compression
Pre-Test	1 mm
Test	0.5 mm
Post-Test	1 mm
Target Mode:	
Distance–Strain	0.5 mm-10%
Trigger Force	0.05 N

Surface Morphological Analysis

SEM was employed in determining the surface morphology of crude PEO and GG, as well as the evidence of the synthesis of semi-IPN within the crosslinked xerogel formulations with the aid of the generated microscopic images. It further assisted in identifying the differences in physical morphology and characteristics of the crude polymers as compared to the crosslinked xerogel. Dried xerogel samples before tableting and native polymers were placed on steel studs and sputter coated with carbon and gold palladium shadowing using the Phenom™ G2 Pro SEM (FEI Company, and Hillsboro, Oregon, USA) by employing various magnifications.

Chemical Composition Study by Fourier Transform-Infrared Spectroscopy (FT-IR)

The FTIR spectra of PEO, GG, and crosslinked semi-IPN xerogel were recorded using an FTIR spectrophotometer (Perkin Elmer Spectrum 100, FT-IR spectrometer) fitted with a universal ATR polarization accessory (Perkin Elmer Ltd., Beaconsfield, UK). Wavelengths were recorded between 4,000 and 650 cm^{-1} and FTIR spectrums of absorbance and % transmittance against distance will be obtained.

Thermal Examination Utilizing Differential Scanning Calorimetry

DSC analysis was conducted for PEO, GG, and the semi-IPN xerogel using a Mettler Toledo, DSC 1, and $STAR^E$ System (Schwerzenbach, Switzerland) at a heating rate of 10°C/min from 25 to 300°C under the constant flow of nitrogen gas. Accurately weighed samples of each (±10 mg) were placed into aluminum sample holders covered and a central pin hole made. Indium metal (99.99%) was used to calibrate the DSC with regards to temperature and enthalpy [16].

Water Content Determination Employing Karl–Fischer Analysis (KF)

KF analysis was conducted for all formulations within the study using the Mettler Toledo V30 Volumetric KF Titrator, with methanol as the moisture standard. Accurately weighed out xerogel samples of 0.01 g were placed within the solvent bath after a baseline drift of zero was achieved, under continuous vigorous stirring with a magnetic stirrer until the titration end point is reached. All samples were tested to determine water content with results obtained in % water content per sample [17].

Powder Flow Characterization Studies

Angle of Repose

The angle of repose is the angle formed between the horizontal bench surface and the cone-shaped mass of powdered xerogel. A glass funnel, 5 cm in height from the base to the orifice was employed. The funnel was secured 4 cm above the bench surface. Thereafter, the powdered xerogel was poured through the funnel orifice, a cone-shaped mass of xerogel formed. The height (h) and radius(r) of the cone-shaped mass were recorded. The angle of repose was thus calculated as follows [18]:

$$\theta = \tan^{-1}(h/r) \tag{3}$$

Carr's Compressibility Index and Hausner Ratio

Bulk (ρbulk) and tapped (ρtap) densities were recorded employing methods as described in the USP. Samples were poured into a 10 mL graduated measuring cylinder with 0.4 mL markings. The bulk density was measured after tapping the cylinder twice on a flat bench top surface. Thereafter, the tapped volume was recorded after tapping in increments of 10, 15, 20, 30, 50, and 100 taps [18]

The recorded bulk and tapped densities were utilized to calculate the Carr's compressibility index (Eq. 4) and Hausner ratio (Eq. 5), respectively.

$$\boldsymbol{CI} = \frac{\boldsymbol{\rho_{tap}} - \boldsymbol{\rho_{bulk}}}{\boldsymbol{\rho tap}} \times 100 \tag{4}$$

$$\boldsymbol{HR} = \frac{\boldsymbol{\rho_{tap}}}{\boldsymbol{\rho_{bulk}}} \tag{5}$$

Swelling and Erosion Studies

A study to evaluate the swelling, erosion, and water uptake characteristics of the tablets was conducted. Whereby the respective tablets were weighed and placed in 250 mL beakers containing 200 mL potassium phosphate buffer pH 6.8 at room temperature and allowed to swell over a 24 h period. Tablets were at predetermined time intervals removed from the buffer and weighed after removing surface water with absorbent tissue paper on a calibrated electronic scale. The swelling ratios, erosion, and water uptake % was calculated using Eqs. 6–10 [19]

$$\text{Swelling Ratio} = \frac{Wt}{Wo}, \tag{6}$$

where *Wt* is the weight of the tablet at time t and *Wo* is the initial weight of the tablet.

$$\text{Dynamic Swelling Ratio}(S) = \frac{Wt - Wo}{Wo}, \tag{7}$$

where *Wt* is the weight at time *t* and *Wo* is the initial weight of the tablet.

$$\text{Water Uptake \%} = \frac{Ws - Wo}{Wo} \times 100, \tag{8}$$

where *Ws* is the weight of the swollen tablet and *Wo* is the weight of the initial tablet.

$$\%\text{Erosion} = \frac{Wo - We}{We} \times 100, \quad (9)$$

where *Wo* is the initial weight of the tablet and *We* is the weight of the test after the erosion test [20]

$$\text{Equilibrium Water Content(EWC\%)} = \frac{Weq - Wo}{Weq} \times 100, \quad (10)$$

where *Weq* is the weight at equilibrium and *Wo* is the weight of the initial tablet [21].

In vitro Drug Release Studies

Dissolution studies were carried out utilizing a USP type II apparatus (Caleva, model 7ST) at 50 rpm and 37°C in 900 mL of potassium phosphate buffer (pH 6.8) with the addition of a stainless steel mesh ring, which fits under the paddle into the lower part of the standard dissolution vessel. Five milliliters of dissolution medium was withdrawn manually at predetermined time intervals during the 24 h study and replaced with an equal volume of fresh dissolution medium to ensure sink conditions were maintained. The samples were then analyzed for drug release via Ultraviolet spectrometry (WinAspect Spectro-analytical software, Analytik Jena AG), at a wavelength of 291 nm employing a calibration curve obtained for the drug [22].

RESULTS AND DISCUSSION

Textural Analysis Studies

Textural analysis data profiles were employed to study the mechanical properties of the crosslinked PEO-GG semi-IPN xerogel matrix tablets in comparison to the PEO-GG blend tablets alone when a uniaxial compression force was applied to the tablets. The work of deformation energy which is calculated as the area under the force-distance curve points to the deformation and rigidity of the tablets. The force-distance curves obtained are the measure of the resistance force encountered by the probe infiltration as a function of the travelled distance into the tablet. A low resistance is depicted by a low slope which further illustrates that the strength of the tablet is low, while a sharp increase in force, a higher slope as the test probe penetrates deeper into the tablet corresponds to a greater strength [23]. From the profiles of force-distance obtained, there was a display of both a high and sharp curve and shorter and less sharp curve when viewed in comparison, thus indicating that the crosslinked PEO-GG semi-IPN xerogel matrix tablets had a greater resistance to the force applied than to the comparative, namely, PEO-GG blend tablets. This may be further highlighted by calculating the gradients of the various force-displacement curves as indicated in Table III, whereby the gradient shows the rigidity of the tablets tested, data indicates that the crosslinked PEO-GG xerogel tablets have an greater rigidity than the PEO-GG blend as a consequence of the new formed polymer chain strength, with Formulation 7 (F7) tablets having the highest rigidity. The same applied for deformation, the crosslinked xerogel tablet showed a lower level of deformity whereas the PEO-GG blend tablet showed the highest value of deformation due to the high binding properties and loose bonds between polymer molecules. The Brinell hardness and resilience of design formulations are represented graphically in Figs. 2 and 3, respectively.

To determine the resilience of the tablets, a strain of 10% was applied to the tablets whereby a textural analysis profile was generated of Force (N)/Time (sec) to the 1:2 and 2:3 ratios, after which the resilience was calculated as depicted in Table III above. From the results obtained, it can be seen that the semi-IPN xerogel matrix tablets F1 have the greatest percentage resilience than its comparatives, which may be attributed to the greater mechanical strength of the crosslinked xerogel due to a greater concentration of crosslinker being used. The data obtained is summarized in Table III. The strain applied as well as the deformation of the xerogel was directly proportional to the compression force applied. In addition, the applied stress and deformation was inversely proportional to the radius and diameter of the indenter probe. This can be confirmed theoretically from the principles of Young's modulus (E) and Eqs. 11–14 [24].

$$\hat{o} = -E(\ddot{e}-1), \quad (11)$$

where $\hat{o}$ is the applied stress and $\ddot{e}$ is the deformation [25]:

$$E^{2/3} = \frac{KF^{2/3}}{R^{1/3}d}, \quad (12)$$

where R is the indenter radius, d is the displacement of the indenter, and F is the compression force. Equating Eqs. 11 and 12, the relations shown in Eqs. 13 and 14 can be deduced.

$$\hat{o} \text{ and } \ddot{e} \propto F \quad (13)$$

$$\hat{o} \text{ and } \ddot{e} \propto 1/R \quad (14)$$

Flow Properties of Powdered-Drug Loaded Xerogel

The angle of repose, Carr's compressibility index, and Hausner ratio were measured for all design formulations, and the results are illustrated in Fig. 4. The angle of repose calculated for all design formulations ranged from 20.48 to 34.4, with majority of the formulations falling within the 20 range. The angle of repose, which is a customary characterization tool used to determine pharmaceutical powder flow. Flowability is based on the angle of repose obtained via the calculation. A value of <30° specifies excellent flow, while values >56° indicates poor flow properties [18]. Based on the results obtained, formulations were rated as having excellent-good flow characteristics

In contrast, the Carr's compressibility (CCI) index and Hausner ratio (HR) were also calculated based on Eqs. 4 and 5. The CCI and HR were found to range from 9–31 to 1.1–1.45, respectively. CCI is a measure of powder bridge strength, and HR is a degree of interparticulate friction. In theory, lower values for CC I and HR, respectively, dictate better flow properties. A CCI value of <10 or HR value of <1.1 is indicated as excellent flow, whereas CCI >38 and HR >1.6 is considered poor flow [26]. Therefore, based on the data obtained, flow of the powdered drug loaded xerogel was rated as excellent-good established by CCI and HR.

Table III. Comprehensive Table of Data Obtained from Textural Analysis Describing the Mechanical Properties of the Semi-IPN Xerogel Matrix Tablets.

Formulation Number	Force (N)	BHN No.	Deformation	Rigidity	Resilience 1:2	Resilience 2:3	Resilience %
F1	46.67	236.00	0.011	96.412	22.821	33.224	145.00
F2	41.43	209.69	0.008	88.945	16.768	9.159	54.62
F3	40.38	204.40	0.008	84.674	17.924	25.776	143.80
F4	39.38	199.00	0.008	83.754	16.743	23.739	141.78
F5	42.67	215.96	0.009	89.565	17.641	27.486	155.81
F6	44.64	225.90	0.010	93.264	21.191	9.452	44.60
F7	48.00	242.94	0.011	101.104	23.317	10.648	45.66
F8	39.41	199.50	0.008	83.607	15.676	8.609	54.92
F9	44.64	225.90	0.010	93.625	19.586	10.733	54.80
F10	48.21	244.00	0.011	101.332	23.730	10.829	45.63
F11	42.86	216.90	0.009	91.720	17.483	9.821	56.17
F12	39.38	199.00	0.008	83.754	16.834	23.846	141.65
F13	42.07	212.93	0.009	87.998	16.814	9.249	55.00
F14	39.68	200.80	0.008	81.759	16.976	7.196	42.39
F15	47.14	238.59	0.011	98.587	21.046	11.575	54.99

Analysis of the Swelling and Erosion Behavior

In this study, the dynamic swelling, in terms of water uptake and erosion of the semi-IPN xerogel and PEO-GG blend tablets, was analyzed by monitoring the change in weight over a predetermined period of time. Figure 5 indicates the percentage of water uptake and thus swelling over a period of time for the varying crosslinked semi-IPN xerogel formulations as well as the PEO-GG blend tablets. The porosity of the polymeric material in question such as GG is a predominant feature that determines its swelling ability. In theory, an increase in porosity leads to greater initial rates of water uptake and a greater level of equilibrium swelling [27]. Porosity affects the rate of dissolution, when a porous polymeric delivery system is placed in direct contact with an aqueous dissolution medium, release of the drug must be headed by dissolution medium penetration into the pores. Pores close to the surface of the matrix become filled with dissolution medium, thus the initial drug diffusion is controlled by the dissolution of drug within the pores [28]. Therefore, the formation of pores within the xerogel system involves the initial penetration of dissolution medium into the pores followed by swelling of the xerogel-pore boundaries thus further prolonging release of drug. Swelling also depends largely on the extent of crosslinking. As seen from Fig. 5, xerogel formulations F1, F7, and F9 have similar swelling characteristics with a uniform delayed swelling behavior ranging between 450 and 500%. Whereas PEO-GG blend shows a constant exponential increase in water uptake and swelling up to and beyond the 24-h test period. Thus, the following observation was made based on swelling test results, the greater the amount of water uptake the greater the degree of erosion due mostly to gellan gum as seen in Fig. 6. Therefore, tablets having a high degree of water uptake were found to erode at a faster rate and thus undergo complete disintegration at an accelerated rate. Although water uptake also encouraged the degree of swelling which mostly relied on the properties of PEO and related to a delayed dissolution and disintegration process. Previous studies have shown that the amount of water uptake is directly proportional to the degree of polymeric erosion; and swelling is controlled by the rate of hydration within dissolution medium. Therefore, extent of matrix swelling and erosion determines drug release kinetics [29]. Visual observations showed that xerogel matrices swell in contact with dissolution medium to form a viscous gel barrier around the core of the tablet. Drug release occurred via this hydrophilic gel barrier; therefore, the rate of release from the matrix is dependent on the viscosity, swelling rate and erosion of the gel layer. It was also noted

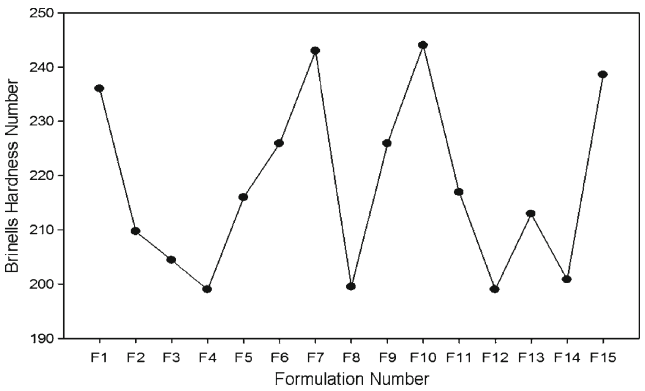

Fig. 2. Diagrammatic representation of Brinells hardness number for Box–Benken statistical formulations depicting the effect of polymer concentration and crosslinking density on the hardness and mechanical strength of formulations

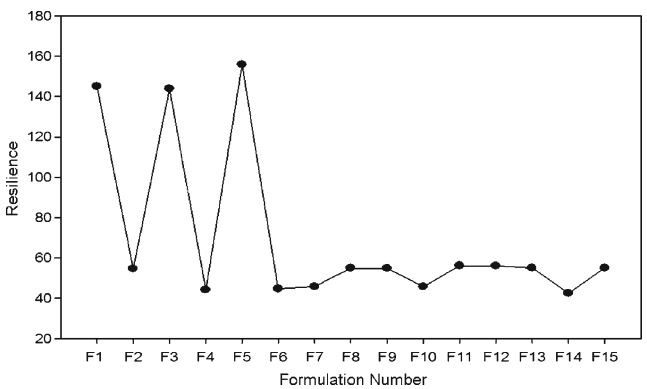

Fig. 3. Illustration of the difference of resilience between all statistical Box–Benken design formulations with variances in chemical composition

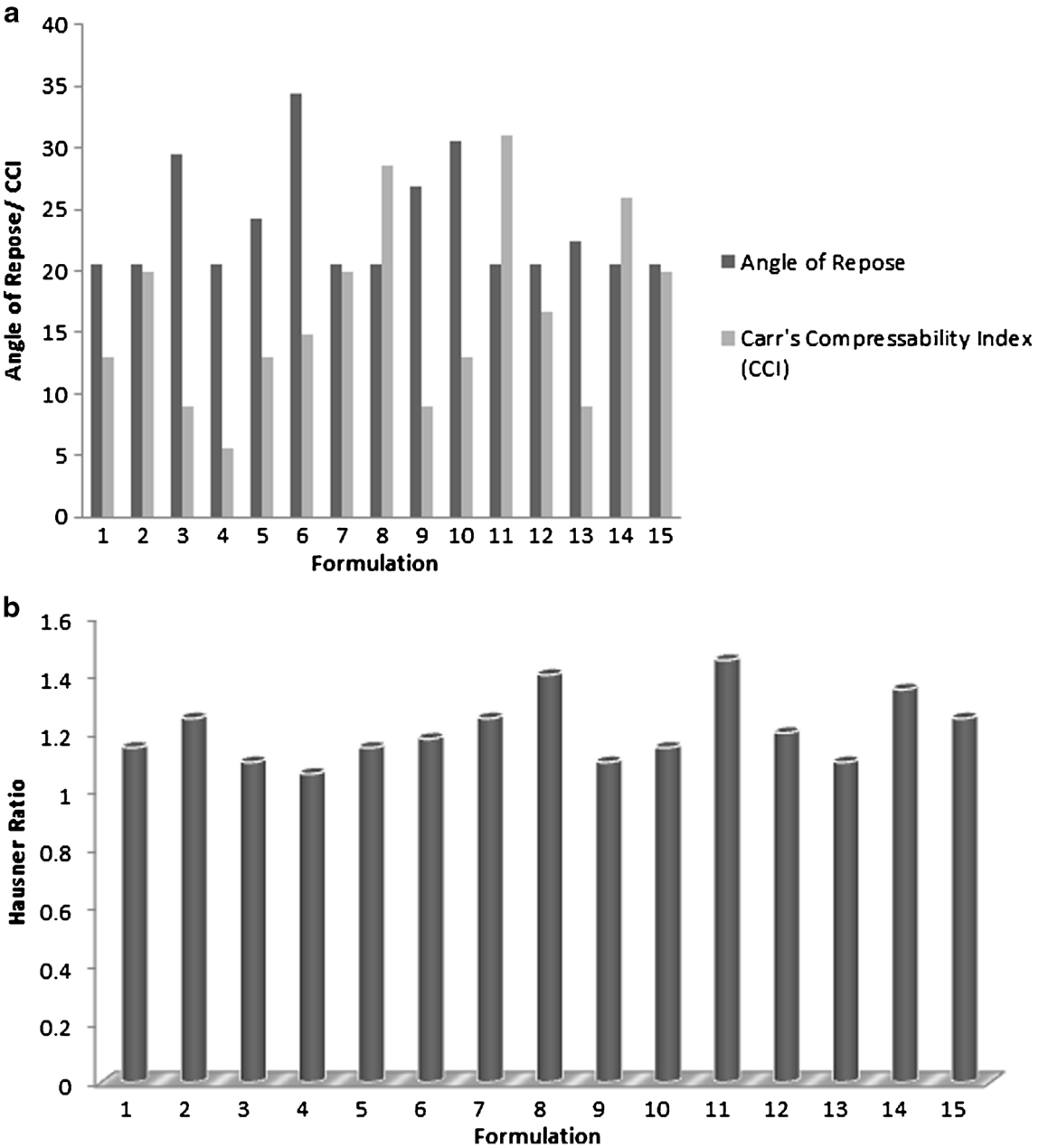

Fig. 4. **a** Graphical illustration of calculated angle of repose and Carr's compressibility index **b** graphical illustration of Hausner ratio

within the study that the swelling of the semi-IPN xerogel was reduced with a corresponding increase in crosslinker concentration, due to the formation of stronger networks. Therefore, the Eq. 15 substantiates this theory.

$$C_c = \frac{1}{Sw}, \tag{15}$$

where *Sw* is the percentage swelling and *Cc* is the concentration of crosslinker.

Hence, by extension, a reduction in crosslinker concentration leads to the formation of looser polymer network or IPN which thus entails the existence of greater hydrodynamic free volume allowing for the absorption of a greater amount of solvent in turn creating a greater swelling capacity [30, 31]. In theory, from the equation of Fick's law of diffusion and the equation for dynamic swelling, we can deduce the relationships shown in Eqs. 16–18 [30].

$$\frac{Mt}{M\infty} = Kt^n, \tag{16}$$

where $\frac{Mt}{M\infty}$ is the fraction of drug released per unit time, *k* is the release constant, and *n* is the release index.

$$\frac{Dt}{D\infty} = Kt^n, \tag{17}$$

where $\frac{Dt}{D\infty}$ is the dynamic swelling, k is the release constant, and *n* is the release index [32]. By equating Eqs. 13 and 14, we find that:

$$\frac{Mt}{M\infty} \propto \frac{Dt}{D\infty}. \tag{18}$$

Therefore, it can be further deduced that the amount of drug released has a strong correlation with the extent of swelling. Furthermore, the amount of drug released at time t is inversely proportional to the overall swelling, hence, with an increase in swelling the drug release at time t, will be reduced, because the drug molecule has to traverse the gel layer before coming into contact with the dissolution medium.

Assessment of the Surface Morphology of the Semi-IPN Xerogel Matrix Tablets

Scanning electron micrograms displayed in Fig. 7 display the surface morphology of pure PEO, GG, and the crosslinked semi-IPN xerogel formulations F1, F7, and F9 after precipitation in acetone and drying under the influence of fume hood. The SEM micrographs show that the semi-IPN xerogel formulations are highly porous as compared to the pure PEO and GG. The average particle size ranged from approximately 240–486 μm. The drastic change in surface morphology between the native polymers and crosslinked semi-IPN xerogels shows that the modification of these polymers was successful. The resultant porous nature of the semi-IPN xerogel furthermore allows for the sustained release of the active from within the interpenetrating network formed. Formulations with a greater degree of crosslinking display a reduced free volume of polymer matrix, which thus delays the passage of drug through the matrix [30, 31].

Karl–Fischer Analysis

The percentage water content was obtained for all design formulations employing a sample size of 0.01 g. Results obtained ranged between 3.149 and 11.454% water content using Eq. 19.

$$\%\,\text{Water Content} = \frac{\text{Volume at Equlibrium(ml)} \times \text{Amount of water in standard(methanol)mg}\Big/\text{mL}}{\text{Weight of sample (mg)}} \times 100\% \tag{19}$$

Formulations depicted varying degrees of water consistency based on the ratio of polymer and crosslinker content. Formulations with an a higher concentration of polymer and crosslinker in overall showed a higher percentage of water content whereas formulations with lower polymer and crosslinker concentrations depicted a reduction in water content. This is possibly due to the greatly hydrophilic nature of PEO and GG, as well as the high degree of water content found in EPI. Ideally, water contact of a solid dosage from should be kept to a minimum due to adverse effects it may have on the physical and chemical characteristics of the product [33]. However, in the current study, it can be seen that although the water content is on the greater spectrum, its mostly due to the chemical nature of the parent polymers and the crosslinking agent used; in addition, characterization studies conducted on the formulations have proven that both the mechanical and chemical components of the system remain satisfactory for a matrix tablet. The water content for design formulations is shown in Fig. 8.

Thermal Analysis of the Crosslinked Semi-IPN Xerogel

Differential scanning calorimetry (DSC) is employed to determine the well as the crystallization temperature of the crude polymers, pure Gelzan™ CM, GG, and pure PEO

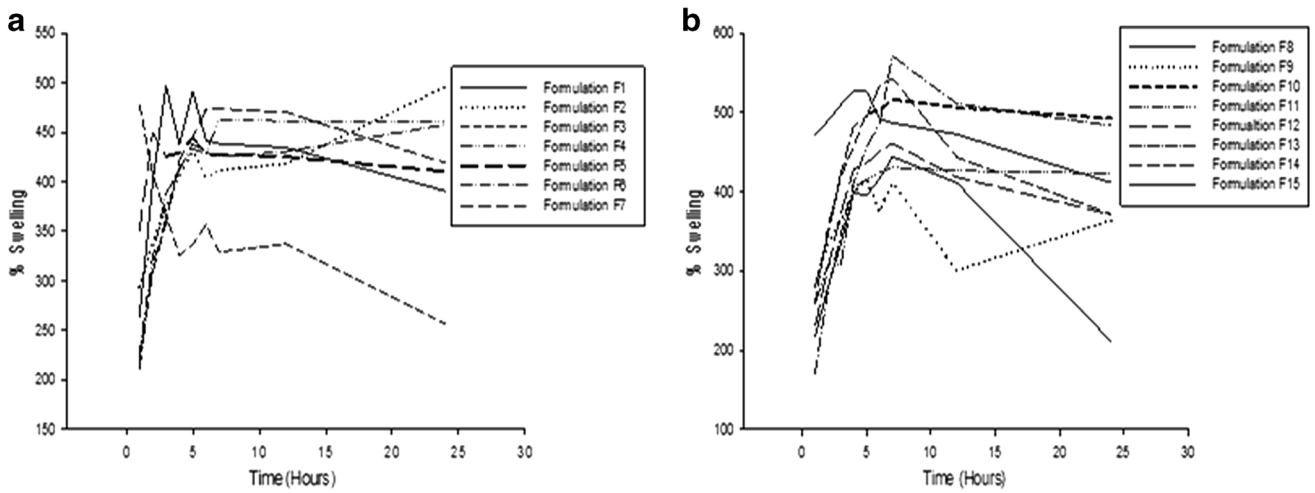

Fig. 5. Graphical representation of swelling (**a** and **b**) characteristics of crosslinked xerogel formulations *versus* a non crosslinked blend to assist in identification of the influence of polymer ratio as well as crosslinker density on the swelling and erosion capabilities of formulations based on chemical variations on exposure to an aqueous environment (pH 6.8)

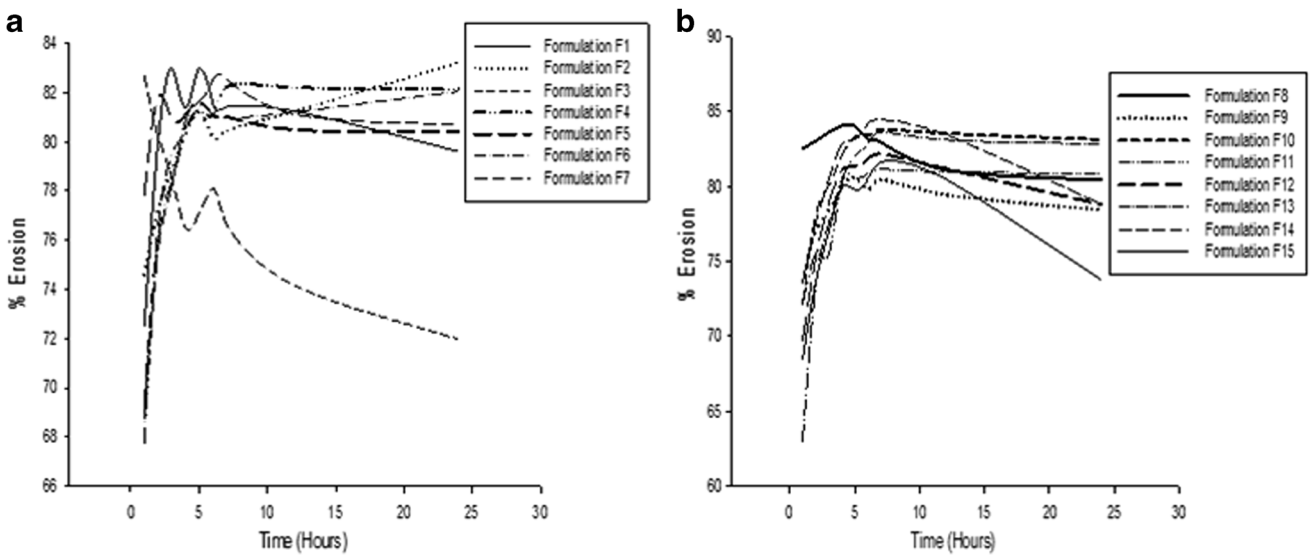

Fig. 6. Graphical illustration of the percentage erosion of design formulations over a 24 h period on exposure to aqueous environment (pH 6.8)

WSR303 as compared to crosslinked semi-IPN xerogel. The procedure follows a thermal analytical method that maintains all test samples at a constant temperature throughout the experimental procedure, whereas the sample temperature holder increases in a linear manner. The DSC thermogram of pure PEO shown in Fig. 9 displays a pronounced endothermic peak at 73.86°C which corresponds to the crystalline melting (Tm) temperature of crude PEO [34]. Glass transition of pure PEO occurs at approximately 65.72°C. An exothermic peak at 190.51°C depicts melting of stable modification. Figure 9 also depicts the thermogram of GG (Gelzan™ CM), shows an endothermic peak at 62.98°C which is due to endothermic peaks only appearing at GG concentrations of 4% and lower with these peaks disappearing at concentrations greater than 8% [35].

The glass transition temperature (Tg) is directly proportional to the crosslinking density, thus as seen in the DSC curves for design formulations it is clearly visible that there is an increase in the Tg with a corresponding increase in the crosslinker concentration ranging between 64.95 and 65.92°C. Melting peaks for all design formulations remained within a stable, constant range between 106 and 107°C; however, there was a slight reduction noted in the melting temperature when the ratio of polymers was reduced, this phenomenon has been described earlier by the Sanchez–Eby theory which states that a reduction in melting temperature is due to a reduction in the heat of fusion present within the reaction, this results because with lower concentrations of polymers there is a greater degree of non-crystallizable units [36]. The melting peaks observed were broad due to the partial crystalline nature of the polymers, this occurs due to the size distribution of crystallites. Melting is then followed by a broad exothermic crystallization peak, the surface of the xerogel which after melting forms a rigid envelope thereby leads to crystallization involves the transition of the polymeric material from a liquid to a crystalline solid, with repeated units forming rigid structure crystallization [37]. It was found that the temperature of crystallization was shifted to higher temperatures with a corresponding increase in crosslinker and polymer concentrations with broad peaks depicting that with an increase in crosslinking the crosslinks appear within the amorphous regions, thus allowing a greater crystalline peak [38]. A prominent crosslinking peak is also noted within the crosslinked semi-IPN xerogel formulations, thus proving the crosslinking reaction of GG-PEO employing epichlorohydrin. This peak is a representative of the crosslinking reaction that occurs upon heating of the sample called curing. These crosslinking peaks are observed with formulations with a higher concentration of crosslinking agent, but absent from those with a reduced crosslinker concentration, most prominent around the temperature of 215°C.

Chemical Structure Stability Evaluation

FT-IR may be used as a 'fingerprint' tool to determine which molecules can differentiate between the xerogel formulations and its precursors such as GG and PEO by using comparisons of known compound consistency. Figure 10 below represents the FTIR spectrum obtained for PEO, GG, and xerogel F1, F7, and F9 as a function of % transmittance against wavelength.

Modifications in chemical structure of the semi-IPN xerogel formulations were analyzed employing FT-IR spectroscopy, which assists in identifying interactions of parent polymers upon chemical reactions such as crosslinking. The current observation of crosslinking was optically detected by noted change in solution viscosity as well as opacity on completion of the crosslinking reaction. The FT-IR spectra of PEO depicted the functional groups present within the chemical compound by determining characteristic bands such as that of O-H functional groups characteristic of alcohols in a range of 3,200–3,600 cm^{-1}, and C≡C stretching depicted at wavenumber range of 2,100–2,260 cm^{-1}. Furthermore, the spectrum for crude GG depicts an important peak at a range of 2,850–2,960 cm^{-1} which corresponds to C-H stretching band [39] and is found in all design formulations as a characteristic GG absorption. On experimental evaluation of the FT-IR data set, it has been inferred that changes in the polymer ratios and crosslinking density have an effect on the vibrational frequencies observed. A broad band in the range of 2,850–

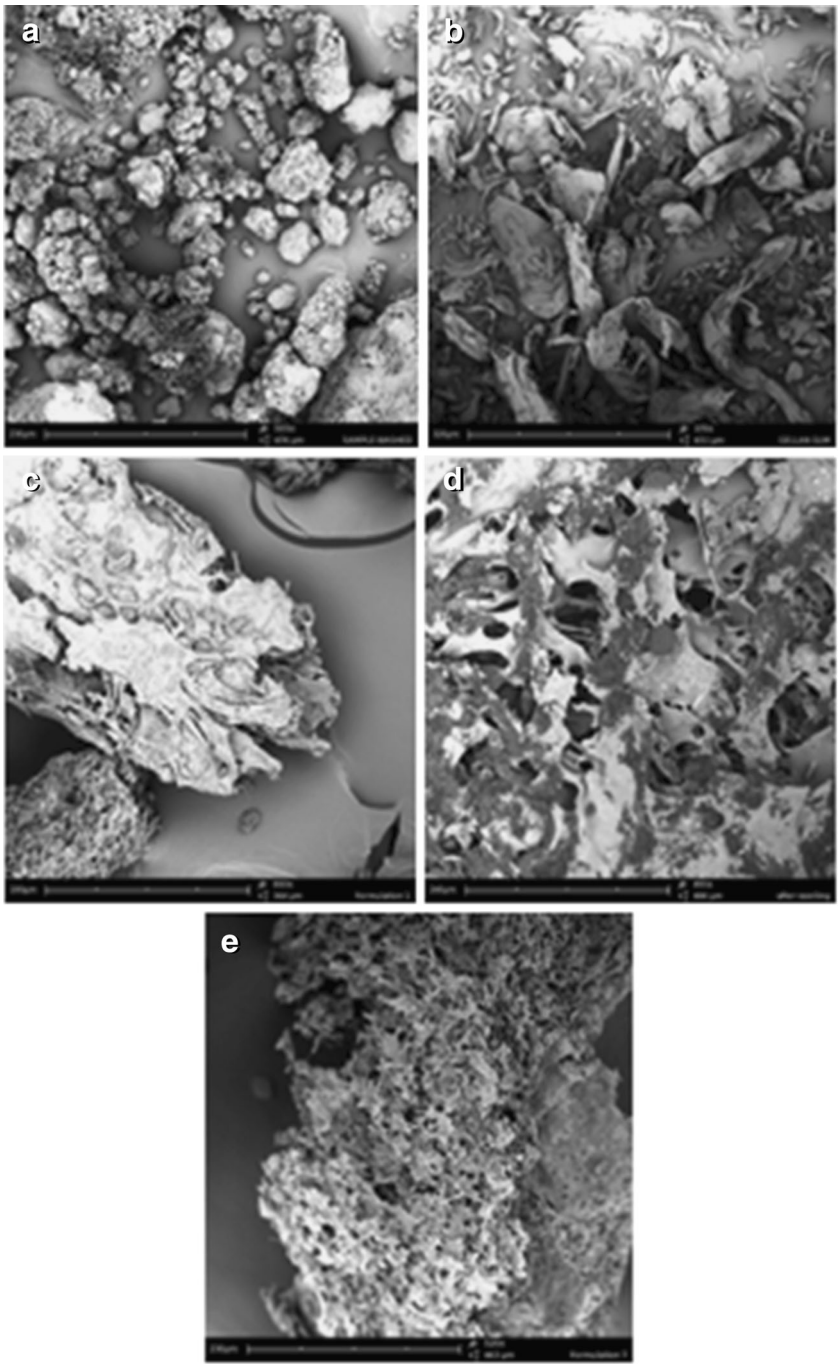

Fig. 7. SEM micrographs of PEO (**a**), GG (**b**), F1(**c**), F7 (**d**), and xerogel F9 (**e**)

2,960 cm^{-1} relating to C-H stretching [39] in alkane functional groups is observed in all semi-IPN xerogel formulations, characteristic of GG.

Due to the presence of NaOH within the crosslinking reaction, it leads to the breakdown of O-H bonds [40] thus causing these hydrogen and oxygen molecules to interact with other molecules, forming new functional groups. This chemical phenomenon leads to the addition of alkene groups with C-H stretching at higher wavelengths of 3,276 cm^{-1} [39], as depicted by the highlighted peak in Fig. 10 of F7. This confers a greater degree of conjugation thereby improving stability and as an extension the physiomechanical properties of the polymer network synthesized. In addition, a strong band relating to the O-H bonding groups within the range of 3,200–3,600 cm^{-1} [39] is observed in semi-IPN xerogels that had an intermediate ratio of polymers relating to the presence of alcohols or phenols. There also exist shifts in the spectrum with the varying crosslinking density. The introduction of N-H amine groups is found in F1, F2, F3, F5, and F10 at a wavelength of 3,360.17 cm^{-1} [39], this is due to the increase in crosslinker density therefore promoting bond formation, the absence of the amino groups within the remaining formulations indicates the absence of amino groups for bonding reactions, this occurrence could be due to the

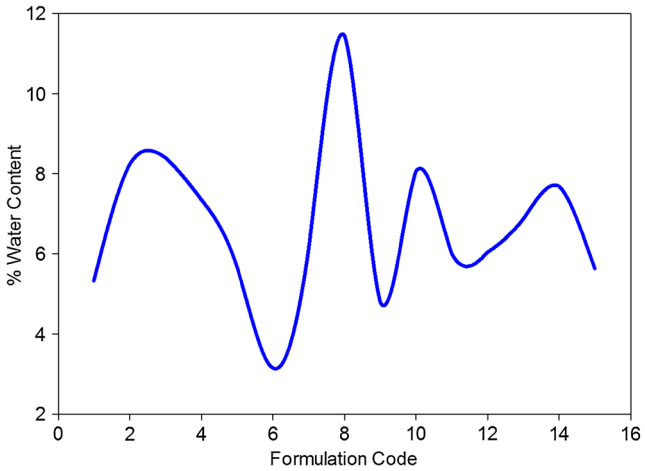

Fig. 8. Graphical illustration of the % Water content results obtained for 15 design formulations employing Karl–Fischer analysis

reduced concentration of GG and increased density of EPI within these formulations which thereby creates steric hindrance.

F9 showed C = C stretch at a wavelength of 1,500 cm^{-1} [39], highlighted in the FT-IR spectra in Fig. 10, which correspond to a conjugational asymmetrical stretch occurring when the ratio of polymers is 1:2.5 and crosslinker is at an intermediate density. C-H stretching within the aromatic ring structure which is derived from the structure of pure GG was observed with all formulations with the resulting incorporation of a C-O functional group within the aromatic structure at a wavelength of 1,080 cm^{-1} [39]. Furthermore, methyl and methylene functional groups were introduced within formulations with a higher concentration of crosslinker due to the introduction of RCH = CH_2 bridges extending from the aromatic ring backbone. Aliphatic ethers represented by wavelengths occurring at 1,060–1,150 cm^{-1} were observed in semi-IPN xerogels that consisted of PEO at a concentration of 1.75%*w/v*. C-N stretching occurred between 1,560 and 1,650 cm^{-1} in formulations that had crosslinking density of 0.6 mL, these peaks tend to occur at higher vibrational frequencies and are known to be associated with the degree of crosslinking [40] and polymer network formation resulting in a change within the structural configuration of the molecules, thus formulations with higher degrees of crosslinking were found to have wavelengths shifting to the greater end of the spectrum. From the data obtained from the FT-IR spectra of all compounds tested, it can be seen that there are distinct changes within the chemical structure with the addition and removal of certain functional groups. Shifting of the aromatic ether occurs in F1, F3, F4, F8, and F11 which all have a crosslinking concentration of 4.4%. There is a disappearance of the C-H in plane bending from xerogel formulations consisting of a polymer ratio of 0.75:1.75%*w/v* thus describing an effect of polymer concentrations of the C-H bonding. Furthermore, individual formulations show characteristically new bands, such as the addition of an alkyne and amine group in F1, as well as methyl groups in F7 and F9.

Chemical crosslinking entails the use of a crosslinking agent to allow a linkage between two polymer chains. The actual crosslinking reaction of both synthetic and natural polymers is accomplished via the reaction between their functional groups with crosslinkers such as Epichlorohydrin. Chemical crosslinking largely implicates the introduction of new functional groups and molecules between the polymeric chains to thereby produce crosslinked chains [41]. This theoretical explanation thus accounts for the additional functional groups and chemical orientation seen in the FT-IR spectra of the crosslinked semi-IPN xerogel formulations as compared to the spectra of PEO and GG. All of the observations help to conclude that polymer concentration as well as crosslinking density has an effect on the formation of semi Interpenetrating networks as observed by peaks within the FT-IR spectra.

In vitro Drug Release Analysis

In order to determine the release profiles of the drug from the hydrophilic matrix tablets, dissolution experiments were performed in accordance with simulated intestinal parameters. The plots of fractional drug release *versus* time for the crosslinked semi-IPN xerogel matrix tablet F1–F5 as well as the PEO-GG blend are depicted in Fig. 11 a–c, respectively. In the case of the crosslinked PEO-GG semi-IPN xerogel formulations drug release was sustained over a period of 24 h, the variation in the concentration of polymers and crosslinker did generate a noticeable deviation in drug release, however, all crosslinked xerogel formulations showed a sustained release over the 24-h study period. Drug delivery from hydrophilic matrix-based systems is controlled by surface erosion of the polymers as well as diffusion of the drug out of the matrix network. Furthermore, erosion is based on the factors such as water uptake and polymer chain lengths [42].

Polymers forming hydrophilic matrices that come into contact with water are known to undergo prompt 'gelification' which is due to the increased size of polymer molecules. There are mainly two mechanisms by which drug release occurs within hydrophilic matrix systems, namely, release by 'controlled swelling', whereby drug undergoes the process of diffusion through the gel layer which is formed as stated above by the swelling or increase in size if polymer chains owing to entry of water, and secondly release by 'controlled dissolution' in which the water gains entry into the system thereby causing 'gelification' of the polymer chains that it comes into contact with; on the other hand, in addition to the conversion of polymer chains to a gel, it also causes the polymer to be dissolved, this therefore involves dissolution or erosion of the polymer.

PEO-GG blends showed drug release behavior with characteristics of both the above mentioned mechanisms, GG was subject to controlled dissolution and thus together with swelling it showed an increase tendency to disintegrate and dissolve thus leading to the initial burst effect in drug release, whereas the following controlled release behavior was mainly based on the properties of PEO which follows controlled swelling mechanisms of drug release, in that polymer chains undergo swelling on contact with aqueous phase due to the vitreous-elastic transition of the polymer been activated, thus the gel layer becomes thicker therefore making the drug release slower, because the drug molecule has to now pass through the thickened gel layer formed by swelling of polymer chains, which is at a greater distance from the surface of the dosage form, which creates a greater resistance to the diffusion of drug

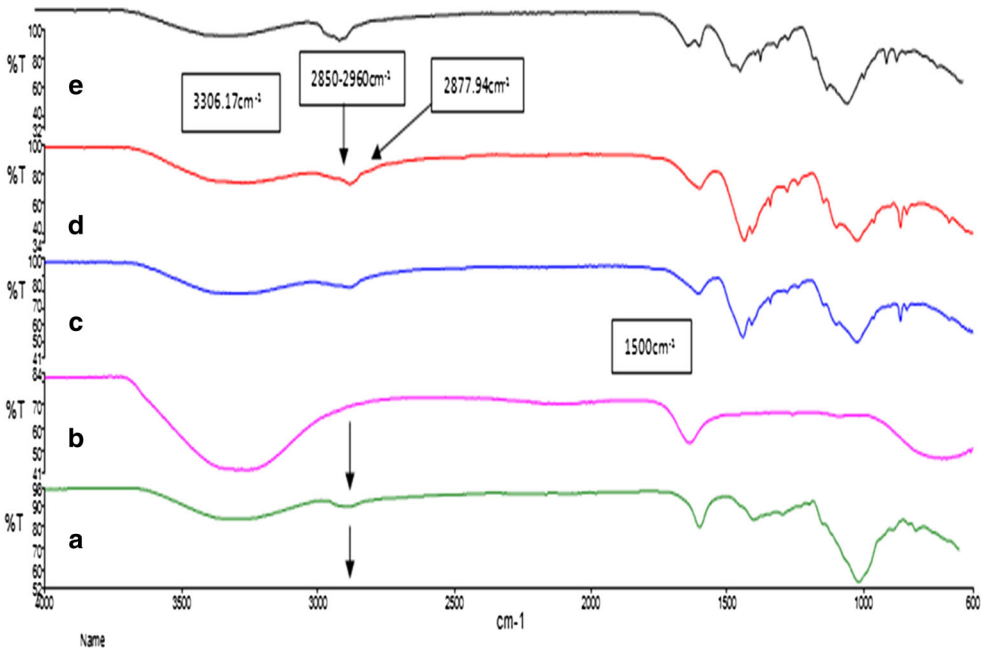

Fig. 9. DSC thermogram of semi-IPN xerogel formulations F1(*c*), F7 (*d*), F9 (*e*), as well as PEO (*b*) and GG (*a*) at a heating rate of 10°C/min from 10–300°C under nitrogen atmosphere

out of the gel layer [43]. Thus drug release from the PEO-GG blend indicated an initial burst effect followed by a rhythmic sustained release above the desired study period of 24 h. Crosslinked PEO-GG semi-IPN xerogels F1–F15 displayed constant sustained release during the 24 h period with 100% drug being released by the end of 24 h, with slight variations in

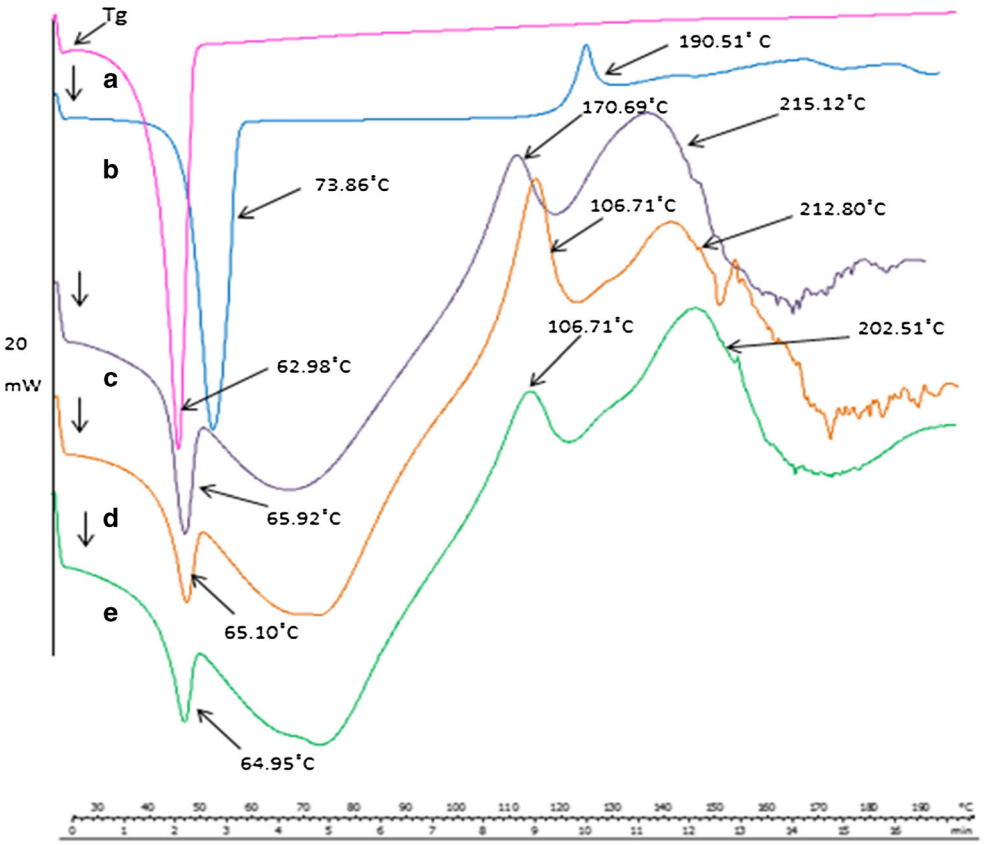

Fig. 10. FTIR spectra of crosslinked semi-IPN xerogel F1 (*f*), F7(**c**), F9 (*d*), as well as pure PEO (*b*) and GG (*a*) depicting the change within chemical structure via the identification of specific functional groups within the spectra obtained. *Pink* and *green spectra* correspond to PEO and GG, respectively, with *black, red* and *blue* representing formulations 1, 7, and 9, respectively

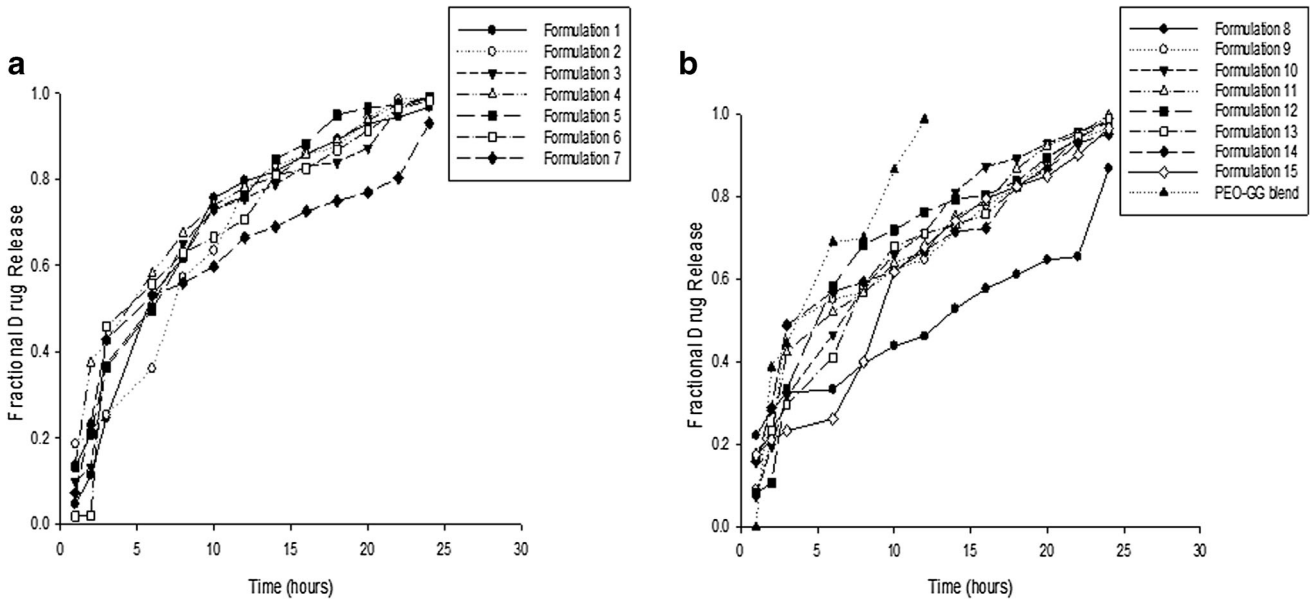

Fig. 11. Graphical illustration of the *in vitro* fractional drug release *versus* time of sustained release semi-IPN xerogel matrix tablets in comparison to release profiles of PEO-GG blend formulations

release rate due to the fact that the swelling and erosion properties of both PEO and GG where modified via the crosslinking reaction, thus these formulations showed a combined mechanism of drug release in terms of 'controlled erosion' and 'controlled dissolution.' From these results, it can be deduced that the higher the crosslinker concentration the greater the modification in drug release, as can be seen in F1 and F9 where a concentration of crosslinker between 0.6 and 0.8 mL is correlated to a greater extent of sustained release, whereas F7, F11, F14, and F15 which has a lower concentration of crosslinker depicts irregular drug release kinetics. It can be proven that the boundary layer thickness is directly proportional to the diffusion of the drug, in addition the tortuosity of the matrix is inversely proportional to the boundary layer thickness. In theory, this can be explicated according to the Levenberg–Marquardt method and Eqs. 20–23 [44].

$$G = \frac{L \times h}{D}, \tag{20}$$

where G is the 'Sherwood number,' D is the diffusion coefficient of the drug, h is the coefficient of the boundary layer, and L is the thickness of delivery system.

$$D' = \left(\frac{D}{\hat{o}}\right), \tag{21}$$

where D is the diffusion coefficient of the drug, $\hat{o}$ is the tortuosity of the diffusion matrix, and D' is the effective diffusion coefficient [45]. By equating Eqs. 16 and 17, the relations shown in Eqs. 18 and 19 can be deduced.

$$h \propto \frac{1}{D'} \tag{22}$$

$$\frac{1}{\hat{o}} \propto h \tag{23}$$

To determine the mechanism of drug release from the xerogel matrix tablet formulations, the data obtained from *in vitro* release studies were applied to the zero-order (cumulative amount of drug released *vs.* time) [46] and Higuchi's (cumulative % of drug released *vs.* square root of time) [18] equation patterns. Release kinetic data for both equations can be seen in Table IV.

When data were plotted in accordance with the zero-order equation, formulations showed linearity, with corresponding regression values ranging between 0.9886 and 0.9926. Release of drug from the matrix system comprising hydrophilic polymers encompasses dynamics of diffusion. Diffusion is responsible for drug passage from the matrix of the system to the dissolution medium subject on a concentration gradient. As the gradient fluctuates, drug is released and the distance for diffusion is increased. Therefore, drug will diffuse at a reduced rate as the distance for diffusion increases, which is denoted as Higuchi kinetics [47].

Table IV. *In vitro* Drug Release Kinetic Data Describing the Mechanism and Order of Sulpiride Release from the Semi-IPN Xerogel Matrix Tablets.

Formulation Code	Zero-order Kinetics Regression Coefficient (R^2)	Higuchi Model Kinetics Regression Coefficient (R^2)
1	0.9879	0.9955
2	0.9924	0.989
3	0.9927	0.9928
4	0.9964	0.9887
5	0.9943	0.9952
6	0.9969	0.9981
7	0.9902	0.9977
8	0.9918	0.9991
9	0.9965	0.9901
10	0.9946	0.9918
11	0.9971	0.9953
12	0.9953	0.9963
13	0.9902	0.9905
14	0.9927	0.9973
15	0.9957	0.9904

Zero order equation, $Q = k_0 t$, Higuchi equation, $Q = k_H t^{1/2}$

Within the context of the current study, *in vitro* profiles of drug release can be elucidated by Higuchi kinetics, as plots showed a great degree of linearity R^2=0.9879–0.9971. However, the comparative complexity of the formulation and its respective constituents may imply that drug release is controlled via more than one kinetic process.

CONCLUSIONS

The study validated that the crosslinking of PEO and GG enhanced the physiochemical and physicomechanical properties of the individual polymers, as well as the formation of a semi-IPN xerogel matrix that allows for sustained drug release. The porous structure of the matrix system further enhanced the ability to achieve sustained drug release.

ACKNOWLEDGEMENTS

This study was funded by the National Research Foundation (NRF) of South Africa.

Conflict on Interest The Authors declare that there are no conflicts of interest.

REFERENCES

1. Dürig T, Fassihi R. Guar-based monolithic matrix systems: effect of ionizable and non-ionizable substances and excipients on gel dynamics and release kinetics. J Control Release. 2002;80:45–56.
2. Huang X, Brazel CS. On the importance and mechanisms of burst release in matrix-controlled drug delivery systems. J Control Release. 2001;73:121–36.
3. Tanaka N, Imai K, Okimoto K, Ueda S, Tokunaga Y, Ibuki R, *et al.* Development of novel sustained-release system, disintegration-controlled matrix tablet (DCMT) with solid dispersion granules of nilvadipine (II): In vivo evaluation. J Control Release. 2006;112:51–6.
4. Shanmugam S, Manavalan R, Venkappayya D, Sundaramoorthy K, Mounnissamy VM, Hemalatha S, *et al.* Natural polymers and their applications. Nat Prod Rad. 2005;4:478–81.
5. Kulkarni VS, Butte KD, Rathod SS. Natural Polymers - A Comprehensive Review. Int J Pharm Biomed Sci. 2012;3:1597–613.
6. Krishnaraj K, Chanrasekar MJN, Nanjan MJ, Muralidharan S, Manikandan D. Development of Sustained release antipsychotic tablets using novel polysaccharide isolated from Delonix regia seeds and its pharmacokinetic studies. Int J Pharm. 2012;20:239–48.
7. Singh A, Sharma PK, Malviya R. Release Behaviour of Drugs from various Natural Gums and Polymers. Polym Med. 2011;41:73–80.
8. Cappello B, DeRosa G, Giannini L. Cyclodextrin containing polyethylene oxide tablets for the delivery of poorly soluble drugs: Potential as buccal delivery system. Int J Pharm. 2006;319:63–70.
9. National Toxicology Program. Report on Carcinogens. 12th Edition, Department of Health and Human Services. 2011; 12:180.
10. Chiba R, Soukura M, Tatsuta S. Liquid Chromatography solid phase extraction and determination of Sulpiride in human serum by high performance liquid chromatography using electro generated chemiluminescence detection. Anal Lett. 2011;44:1559–69.
11. Barnes TRE, Davison S, Ferrier IN, et al. Consensus statement on high dose Anti-psychotic medication. Royal College of Psychiatrics. 2006;1-51.
12. Watanabe K, Sawano T, Terada K, Endo T, Sakata M, Sato J. Studies on Intestinal Absorption of Sulpiride (1): Carrier-Mediated Uptake of Sulpiride in the Human Intestinal Cell Line Caco-2. Biol Pharm Bull. 2002;25:885–90.
13. Sigma Aldrich, MDS (±) Sulpiride, Germany.
14. Covielloa T, Alhaiquea F, Parisia C, Matricardia P, Bocchinfusob G, Grassi M. A new polysaccharidic gel matrix for drug delivery: preparation and mechanical properties. J Control Release. 2005;102:643–56.
15. Choonara YE, Pillay V, Carmichael T, Danckwerts MP. An in vitro study of the design and development of a novel doughnut-shaped Minitab let for intraocular implantation. Int J Pharm. 2006;310:15–24.
16. Kreye F, Hamm G, Karrout Y, Legouffe R, Bonnel D, Siepmann F, *et al.* MALDI-TOF MS imaging of controlled release implants. J Control Release. 2012;161:98–108.
17. Scaccia S. Water determination in composite PEO-based polymer electrolytes by volumetric Karl Fischer titration method. Talanta. 2005;67:678–81.
18. Shah RB, Tawakkul MA, Khan MA. Comparative Evaluation of Flow for Pharmaceutical Powders and Granules. AAPS PharmSciTech. 2008;9:250–8.
19. Özeroglu C, Birdal A. Swelling properties of acrylamide-N, N′-methylene bis (acrylamide) hydrogels synthesized by using meso-2, 3-dimercaptosuccinic acid-cerium (IV) redox couple. Express Polym Lett. 2009;3:168–76.
20. Reddy MM, Reddy JD, Moin A, Shivakumar HG. Formulation of Sustained –Release Matrix Tablets using Crosslinked Karaya Gum. Trop J Pharm Res. 2012;11:28–35.
21. Murthy PSK, Mohan YM, Sreeramulu J, Raju KM. Semi IPNs of starch and poly (acrylamide-co-sodium methacrylate): Preparation, swelling and diffusion characteristics evaluation. J Reac Funct Polym. 2006;66:1482–93.
22. Strübing S, Metz H, Mäder K. Characterization of poly (vinyl acetate) based floating matrix tablets. J Control Release. 2008;126:149–55.
23. Pillay V, Fassihi R. A novel approach for constant rate delivery of highly soluble bioactives from a simple monolithic system. J Control Release. 2000;67:67–78.
24. Ruvalcaba AM, Snchez-Diaz JC, Becerra F, Cruz-Barba LE, Gonzalez-Alvarez A. Swelling characterization and drug delivery kinetics of polyacrylamide-co-itaconic acid/chitosan hydrogels. Express Polym Lett. 2009;3:25–32.
25. Khalid MN, Agnely F, Yagoubi N, Grossiord JL, Couarraze G. Water state characterization, swelling behaviour, thermal and mechanical properties of chitosan based networks. Eur J Pharm Sci. 2002;15:425–32.
26. Aulton ME. The Design and Manufacture of Medicines. Third Edition. Philadelphia. Elsevier. 2007;109–110.
27. Ferrero C, Massuelle D, Deolker E. Towards elucidation of the drug release mechanism from compressed hydrophilic matrices made of cellulose ether. II Evaluation of a possible swelling-controlled drug release mechanism using dimensionless analysis. J Control Release. 2010;141:223–33.
28. Ahuja G, Pathak K. Porous carriers for controlled/modulated drug delivery. Ind J Pharm Sci. 2009;71:599–607.
29. Sriamornsak P, Thirawong N, Weerapol Y, Nunthanid J. Swelling and Erosion of pectin Matrix tablets and their impact on drug release behaviour. Eur J Pharm Biopharm. 2007;7:211–9.
30. Kulkarni RV, Baraskar VV, Setty CM, Sa B. Interpenetrating Polymer Network Matrices of Sodium Alginate and Carrageenan for Controlled drug delivery application. J Fibres Polym. 2011;12:352–8.
31. Kulkarni RV, Mangond BS, Mutalik S, Sa B. Interpenetrating polymer network microcapsules of gellan gum and egg albumin entrapped with diltiazem–resin complex for controlled release application. Carb Polym. 2011;83:1001–7.
32. Rokhade AP, Agnihotri SA, Patil SA, Malikarjuna NN, Kulkarni PV, Aminabhavi TM. Semi- Interpenetrating polymer network microspheres of gelatin and sodium Carboxymethyl cellulose for controlled release of ketorolac tromethamine. Carb Polym. 2006;65:243–52.
33. Szakonyi G, Zelkó R. The effect of water on the solid state characteristics of pharmaceutical excipients: Molecular mechanisms,

measurement techniques, and quality aspects of final dosage form. Int J Pharm Invest. 2012;2:18–25.
34. Ibrahim S, Johan MR. Thermolysis and Conductivity Studies of Poly (Ethylene Oxide) (PEO) Based Polymer Electrolytes Doped with Carbon Nanotube. Int J Electrochem Sci. 2012;7:2596–615.
35. Izumi Y, Saito S, Soma K. Differential Scanning Calorimetry and Structural studies of the sol-gel transition of gellan gum in water. Progress Colloid Polym Sci. 1999;114:48–55.
36. Zo-li JTU. Morphology, Crystallization and Melting Behavior of Propylene-Ethylene Statistical Copolymers. Doctor of Philosophy. Virginia: Polytechnic Institute and State University. 2005;3–29.
37. UserCom, 1/2000, Information for users of METTLER TORLEDO thermal analysis systems, Mettler Toledo. 2000;1–25.
38. Reis MD, Pruitt L. Effects of cross-linking on the microstructure and mechanical properties of ultra- high molecular weight. Clin Orthopedic Res. 2005;440:149–56.
39. Coates J. Interpretation of Infrared Spectra, A Practical Approach. In. Encyclopedia of Analytical Chemistry. R.A. Meyers (Ed.) 2000; pp. 10815–10837.
40. Adel AM, Abou-Youssef H, El Gendy AA, Nada AM. Carboxymethylated Cellulose Hydrogel Sorption, Behaviour, and Characterization. Nature Sci. 2010;8:244–56.
41. Gulrez SKH, Al-Assaf S, Phillips GO. Hydrogels: Methods of Preparation, characterization and Applications. In. Progress in Molecular and Environmental Bioengineering - From Analysis and Modeling to Technology Applications. A. Carpi (Ed.) 2011; pp. 307–568.
42. Toti US, Aminabhavi TM. Modified guar gum matrix tablet for controlled release of diltiazem hydrochloride. J Control Release. 2004;95:567–77.
43. Maderuelo C, Zarzuelo A, Lanao JM. Critical factors in the release of drugs from sustained release hydrophilic matrices. J Control Release. 2011;154:2–19.
44. Siepmann J, Lecomte F, Bodmeie R. Diffusion- controlled drug delivery systems: calculation of the required composition to achieve desired release profiles. J Control Release. 1999;60:379–89.
45. Siepmann J, Peppas NA. Modeling of drug release from delivery systems based on hydroxypropyl methylcellulose (HPMC). J Adv Drug Del Rev. 2012;64:163–74.
46. Shoaib MH, Tazeen J, Merchant HA, Yousuf RI. Evaluation Of Drug Release Kinetics From Ibuprofen Matrix Tablets Using HPMC. Pak J Pharm Sci. 2006;19:119–24.
47. Reddy KR, Mutalik S, Reddy S. Once-Daily Sustained-Release Matrix Tablets of Nicorandil: Formulation and In Vitro Evaluation. AAPS PharmSciTech. 2003;4:1–9.